Complete analysis of the angular momentum distribution of molecules desorbing from a surface

S. Borowski, T. Klüner,[a] and H.-J. Freund

Fritz-Haber-Institut der Max-Planck-Gesellschaft, Faradayweg 4-6, 14195 Berlin, Germany

We theoretically analyze the angular momentum distribution of molecules desorbing from a surface. The adsorbate is shown to possess the complete point symmetry of the surface if the molecules adsorb in statistically equilibrated local order. Considering the symmetry of the angular momentum distribution, this point symmetry adopted to the desorbate is particularly taken into account. From the symmetry analysis, the cancellation of several terms in the angular momentum distribution is concluded. The symmetry related sparseness of the angular momentum distribution strongly simplifies the interpretation of experimental data and thus enables an appropriate comparison between experiment and theory. The benefit of this simplified picture is demonstrated by the example of the laser induced desorption of CO molecules from a $Cr_2O_3(0001)$ surface. © *2003 American Institute of Physics.* [DOI: 10.1063/1.1618212]

I. INTRODUCTION

Experimental investigations on orientation and alignment in the dynamics of molecules on surfaces[1–10] have been a focus in surface science since spatial characteristics of molecular dynamics became accessible by rapid developments of laser spectroscopy.[11] By detecting the molecules via REMPI (resonance enhanced multiphoton ionization) or LIF (laser induced fluorescence), orientation and alignment parameters are extracted from the angular momentum distribution of the molecules to describe the rotational motion in the molecular dynamics.[12–14]

Concerning measurements of spatial orientation and alignment, however, laser probe techniques have an initrinsic limit: The electric field vector of the laser pulse is constrained to the plane perpendicular to the propagation direction. Thus, the angular momentum distribution is only projected onto ''apparent'' instead of real orientation and alignment parameters because their line strength factors become linearly dependent in the plane probed by the electric field vector.[12–14] The apparent parameters are linear combinations of real parameters with coefficients that depend on the detection geometry, the transition branches, and the polarization of the laser pulse. To reveal the specific features of the molecular rotational motion depicted by the real parameters, this linear combinations have to be disentangled. Experimentally, the real parameters can be determined from the apparent parameters either by employing different detection geometries or by using several transition branches and polarizations.

Since both opportunities require a significant effort, most experimental studies usually rely on the reasonable assumption that the investigated system is cylindrically symmetric with regard to the surface normal.[2,3,5–10] Then, the off-axial orientation and alignment parameters become zero and the angular momentum distribution is only composed of the remaining axial parameters. This restriction results in much simpler linear combinations relating the apparent to the real parameters. Employing appropriate experimental setups (detection geometry and polarization), the apparent and real parameters are even coincident. Hence, a straight measurement of real axial parameters is possible in case of cylindrical symmetry. However, the assumption of cylindrical symmetry about the surface normal and thus a strictly flat surface has never been quantitatively scrutinized in detail. Only qualitative or semiquantitative arguments to support this simplification can be found in literature for a few systems investigated.[3,5] Consequently, the data analysis of orientation and alignment measurements still poses a difficult problem.

For studies on desorption processes, the present paper introduces a new aspect to the discussion about the disentanglement of the real parameters contained in the apparent parameters: Surface symmetry that is introduced to the angular momentum distribution of desorbates via the previous adsorbed state of the molecules. The consequences of such symmetry for the orientation and alignment parameters are completely derived within a density matrix description. The resulting symmetry consideration is illustrated by the exhaustive theoretical analysis of the angular momentum distribution of CO molecules photodesorbing from a $Cr_2O_3(0001)$ surface.

The paper is structured as follows: In Sec. II, we discuss how surface symmetry is taken over to the adsorbate. Section III reviews the general representation of angular momentum distributions in terms of state multipoles. In Sec. IV, the representation of angular momentum distributions of desorbates is considered with reference to the symmetry adopted from the surface. The symmetry transformation behavior of the orientation and alignment parameters is derived. Section V presents the application of this symmetry analysis to experimental an theoretical studies of the laser induced desorption of CO from $Cr_2O_3(0001)$. Ultimately, we conclude in Sec. VI.

[a]Electronic mail: kluener@fhi-berlin.mpg.de

10367

10368   J. Chem. Phys., Vol. 119, No. 19, 15 November 2003

Borowski, Klüner, and Freund

II. SYMMETRY OF ADSORBATE-SUBSTRATE COMPLEX

To characterize the symmetry of surfaces, the general Group Theoretical description is provided in terms of two-dimensional space groups.[15] In case of planar objects like surfaces, symmetry operations are restricted to rotations about axes normal to the plane and reflections in mirror lines laying in the plane. Due to translational symmetry glide reflections in glide lines may also be included.

Every two-dimensional space group belongs to a corresponding point group. Thus, along with the two-dimensional space group classification a general surface is also assigned to a point group $\mathbf{G}_{sur}$ of order h_{sur} that contains the complete point symmetry of the surface. If a single molecule is adsorbed on the surface, the adsorption site is singled out and the translational symmetry is broken. Hence, the two-dimensional space group of the surface is reduced to a local point group $\mathbf{G}_{loc} \subseteq \mathbf{G}_{sur}$ of order h_{loc} that describes the *local symmetry* of the adsorbate. In the realistic case, however, a large number of molecules is adsorbed on the surface forming an adsorbate ensemble. If the local symmetry of the adsorbate does not include the complete point symmetry of the surface, that is $\mathbf{G}_{loc} \subset \mathbf{G}_{sur}$, equivalent adsorption sites are provided by the surface due to its heretofore unconsidered point symmetry. Assuming that the surface is well-ordered and the molecules adsorb in statistically equilibrated local order, these equivalent adsorption sites are occupied by the adsorbing molecules with equal probability. Then, the adsorbate additionally shows an *ensemble symmetry* in the statistical limit. Group Theoretically, such adsorbate ensemble is described by a decomposition

$$\mathbf{G}_{sur} = \mathbf{G}_{loc} + a_{ens}^2 \mathbf{G}_{loc} + \cdots + a_{ens}^n \mathbf{G}_{loc}, \tag{1}$$

of the surface point group $\mathbf{G}_{sur}$ into cosets with respect to the local point group $\mathbf{G}_{loc}$ of the adsorbate.[16,17] The $n = h_{sur}/h_{loc}$ cosets represent the equivalent adsorption sites. The symmetry operations a_{ens}^i $(i=1,\ldots,n)$ of the ensemble symmetry map the equivalent adsorption sites onto each other. For the trivial coset $\mathbf{G}_{loc}$ in Eq. (1), the identity operation $a_{ens}^1 = E$ is omitted. Consequently, the complete point symmetry of the surface is introduced to the adsorbate and thus to observables of macroscopic methods that evenly average over all adsorption sites and do not violate this symmetry themselves.

An adsorbate on a surface may show both local and ensemble symmetry with respect to rotation since the point group $\mathbf{C}_f$ of an f-fold rotational symmetry can contain proper subgroups. With regard to reflection, however, the adsorbate can only exhibit either local or ensemble symmetry because the point groups $\mathbf{C}_s^{(i)}$ $(i=1,\ldots,f)$ related to the f-fold rotational axis possess no proper subgroups.

By way of example, Fig. 1 shows CO molecules adsorbed on a $Cr_2O_3(0001)$ surface.[18,19] The polar metal oxide surface is stabilized by half Cr ion termination.[19] Neglecting the asymmetry of the Cr ions in the lower layers, the surface exhibits trigonal p31m space symmetry (Hermann–Mauguin notation) which belongs to C_{3v} point symmetry (Schoenflies notation). The CO molecules adsorb in flat bonding geometry inline with two surface Cr ions.[18] Hence, a single CO
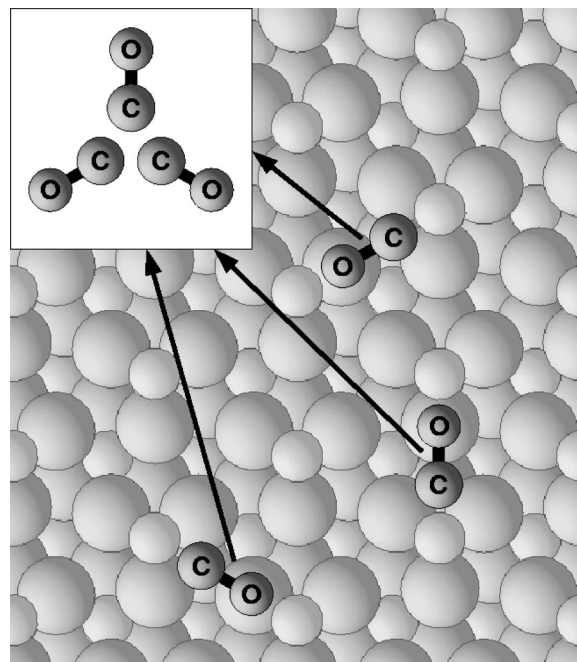

FIG. 1. CO–$Cr_2O_3(0001)$ with $C_s^{(1)}$ local symmetry and C_3 ensemble symmetry of the CO adsorbate (Ref. 18).

molecule adsorbed on a $Cr_2O_3(0001)$ surface shows $C_s^{(1)}$ local symmetry. Moreover, a CO adsorbate ensemble on aforementioned premises consists of three differently orientated equivalent kinds of molecules resulting in a C_3 ensemble symmetry. The Group Theoretical description of this CO adsorbate ensemble is given by the decomposition

$$\mathbf{C}_{3v} = \mathbf{C}_s^{(1)} + C_3 \mathbf{C}_s^{(1)} + C_3^2 \mathbf{C}_s^{(1)}, \tag{2}$$

of the surface point group $\mathbf{C}_{3v}$ in cosets of the local point group $\mathbf{C}_s^{(1)}$ via the rotation operations $\{C_3^0 = E, C_3^1, C_3^2\}$ of the ensemble symmetry. Consequently, the complete point symmetry of the $Cr_2O_3(0001)$ surface is recovered for the CO adsorbate.

III. GENERAL STATE MUTLIPOLE EXPANSION

To discuss the orientation and alignment of a single isolated molecule, we use an established density matrix description.[20] For a definite j state of angular momentum $\hat{\mathbf{J}}$, the geometrical characteristics of the angular momentum vector is determined by the population distribution and the coherence relation of the different states $-j \leq m \leq j$ of the angular momentum projection $\hat{J}_z$. Hence, the density matrix of a given state $|\psi\rangle$ in the basis states $\{|jm\rangle\}$

$$\rho_{m'm} = \langle jm'|\psi\rangle\langle\psi|jm\rangle, \tag{3}$$

is to be analyzed for a specific angular momentum state j. In the paper on hand, the population of all j states is assumed to equal unity. Therefore, all occurring density matrices are normalized. Following Orr-Ewing and Zare,[21] we expand the density matrix

$$\rho_{m'm} = \sum_{kq} \rho_q^{(k)} \langle jm'|\hat{T}_q^{(k)}|jm\rangle, \tag{4}$$

in terms of state multipoles $\hat{T}_q^{(k)}$, that are spherical tensor operators of rank $k \geq 0$ and component $-k \leq q \leq k$.[20,22] Then, the expansion coefficients resulting from the orthogonality of the state multipoles

$$\rho_q^{(k)}(j) = \sum_{mm'} \rho_{m'm} \langle jm' | \hat{T}_q^{(k)} | jm \rangle, \tag{5}$$

are referred to as state multipole moments. The matrix elements of the state multipoles are resolved by application of the Wigner–Eckardt theorem

$$\rho_q^{(k)}(j) = \sum_{mm'} \rho_{m'm} (-1)^{j-m'} (j\|T^{(k)}\|j) \begin{pmatrix} j & k & j \\ -m' & q & m \end{pmatrix}, \tag{6}$$

with the reduced matrix elements $(j\|T^{(k)}\|j) = \sqrt{2k+1}$. The emerging 3-j symbols vanish unless the triangle condition

$$0 \leq k \leq 2j \quad \text{and} \quad m' = q + m, \tag{7}$$

is satisfied. Thus, Eq. (5) can formally be rewritten

$$\rho_q^{(k)}(j) = \sum_{mm'} \rho_{m'm} T_q^{(k)}(j,m) \delta_{m',m+q}$$

$$= \sum_m \rho_{m+q,m} T_q^{(k)}(j,m), \tag{8}$$

where all state multipole moments with $k > 2j$ become zero and $T_q^{(k)}(j,m)$ is a symmetry adapted notation for the nonvanishing matrix elements of the state multipoles. Hence, only the qth sub/superdiagonal of the density matrix contributes to the state multipole moments of component q. In this regard, the zeroth sub/superdiagonal denotes the main diagonal containing the populations of the m states. The qth sub/superdiagonals with $q \neq 0$ describe the coherence relation between the m states.

In common studies,[1–10,23–29] however, the angular momentum polarization is preferably investigated in reference to the well-known orientation and alignment parameters

$$A_q^{(k)}(j) = \frac{c(k)}{[j(j+1)]^{k/2}} \sum_{mm'} \rho_{m'm} \langle jm | \hat{J}_q^{(k)} | jm' \rangle. \tag{9}$$

Similarly, these quantities are obtained as coefficients from an equivalent expansion of the density matrix in terms of angular momentum tensors $\hat{J}_q^{(k)}$.[12,13] The normalization constants $c(k)$ are determined according to the predefinition of the high-j limit behavior of the axial parameters $A_0^{(k)}$: The axial parameters generally coincide with the Legendre polynomial $P_k(J_z/J)$ integrated over the angular momentum distribution except for $k = 2$ where the asymptote is twice the usual quantity.[13] The orientation parameters (with odd rank) describe a polarization of the angular momentum vector $\hat{\mathbf{J}}$ involving its direction sign. A polarization of the angular momentum vector $\hat{\mathbf{J}}$ irrespective of its direction sign is described by the alignment parameters (with even rank).[21] The angular momentum tensors $\hat{J}_q^{(k)}$ are spherical tensor operators as well as the state multipoles $\hat{T}_q^{(k)}$. Then, the Wigner–Eckardt theorem states that only their reduced matrix ele-

ments differ whereas the geometrical properties given by the 3-j symbols are the same. Consequently, the orientation and alignment parameters

$$A_q^{(k)}(j) = \frac{c(k)}{[j(j+1)]^{k/2}} \sum_{mm'} \rho_{m'm} J_q^{(k)}(j,m') \delta_{m,m'+q}$$

$$= \frac{c(k)}{[j(j+1)]^{k/2}} \sum_{m'} \rho_{m',m'+q} J_q^{(k)}(j,m'), \tag{10}$$

can be transformed in the same way as the state multipole moments. Again, all parameters with $k > 2j$ vanish and the quantities $J_q^{(k)}(j,m')$ denote the corresponding nonzero matrix elements. Here, the only contribution to the parameters of component q is given by the qth super/subdiagonal of the density matrix.

Finally, the equivalence of the introduced representations of the density matrix can be expressed by the relationship

$$A_q^{(k)}(j) = \frac{c(k)}{[j(j+1)]^{k/2}} \frac{(j\|J^{(k)}\|j)}{(j\|T^{(k)}\|j)} (-1)^q \rho_{-q}^{(k)}(j), \tag{11}$$

connecting the orientation and alignment parameters and the state multipole moments. This is a direct result of the Wigner–Eckardt theorem relating Eqs. (5) and (9) to each other by the quotient of the reduced matrix elements. In contrast to the simple form of the reduced matrix elements of the state multipoles, the reduced matrix elements $(j\|J^{(k)}\|j)$ of the angular momentum tensors have a more complicated structure. Explicit expressions up to rank $k = 4$ can be found in Ref. 22, a general expression is given in Ref. 30.

IV. ORIENTATION AND ALIGNMENT PARAMETERS FOR DESORBATES

The characteristics of molecules desorbing from a surface, for example the angular momentum polarization, are determined by the desorption process and the preceding adsorbed state of the molecules. In general, the desorption process does not violate the symmetry of the adsorbate. However, the macroscopic detection of the desorbate evenly averages over the microscopic lateral positions of the previously adsorbed molecules on the surface. Therefore, the point symmetry of the adsorbate is further imposed on the ensemble of desorbing molecules. Provided the adsorbed state of the molecules possesses statistically equilibrated local order, this symmetry amounts to the complete point symmetry of the surface (see Sec. II). In the following, we investigate the consequences of such point symmetry for the orientation and alignment parameters of the desorbate. Henceforth, the surface normal is assigned to the z axis. The lateral coordinates x and y are only set if necessary.

A. Rotational symmetry

A given ensemble of desorbing molecules is described by an incoherent superposition of the individual molecule states. Concerning rotational symmetry, this desorbate ensemble shows the local symmetry of a single molecule adsorbed on the surface. Furthermore, the desorbate exhibits an

ensemble symmetry with respect to molecule mixtures that arise from differently orientated equivalent adsorption sites (see Sec. II).

For f-fold local symmetry and F-fold ensemble symmetry, the resulting density matrix of the desorbate in the basis $\{|jm\rangle\}$ is given by

$$\rho_{m'm}^{\text{des}} = \frac{1}{F}\sum_{N=0}^{F-1} \langle jm'|\hat{\rho}^N|jm\rangle = \frac{1}{F}\sum_{N=0}^{F-1} \rho_{m'm}^N, \qquad (12)$$

with the density operators $\hat{\rho}^N$ and the density matrices $\rho_{m'm}^N$ describing the orientated molecule mixtures. Because of the local symmetry of every single molecule, the rotation $\hat{C}_f$ leaves the density matrices

$$(\rho_{m'm}^N)' = \langle jm'|\hat{C}_f^\dagger \hat{\rho}^N \hat{C}_f|jm\rangle, \qquad (13)$$

of the orientated molecule mixtures unchanged. Considering the representation of the unitary rotation operator $\hat{C}_f = \exp[-2\pi i \hat{J}_z/f]$ in the basis states $\{|jm\rangle\}$, this expression is transformed into

$$(\rho_{m'm}^N)' = \exp\left[\frac{2\pi i}{f}(m'-m)\right]\rho_{m'm}^N. \qquad (14)$$

To satisfy the required identity of the transformed and the original density matrices, either the exponential factor equals unity or the particular density matrix element becomes zero. Hence, the density matrix elements vanish until $m'-m = nf$ with an integer n is fulfilled. Then, the density matrices can be rewritten

$$\rho_{m'm}^N = \sum_d \rho^N(m,d)\delta_{m'-m,d}\delta_{d,nf}, \qquad (15)$$

with $\rho^N(m,d)$ denoting the mth element of the dth sub/superdiagonal of the density matrices. Obviously, the sub/superdiagonals vanish if their index is not a multiple of the local foldness.

On account of the ensemble symmetry of the desorbate, the equivalent density operators in Eq. (12) can be transformed into each other by successive operation of the rotation $\hat{C}_F = \hat{C}_F^1$. Thus, the density matrix of the desorbate ensemble is further evaluated to

$$\rho_{m'm}^{\text{des}} = \frac{1}{F}\sum_{N=0}^{F-1} \langle jm'|\hat{C}_F^{F-N}\hat{\rho}^0\hat{C}_F^N|jm\rangle, \qquad (16)$$

where all involved density operators are expressed by the accordingly rotated reference density operator $\hat{\rho}^0$. The adjoint of the rotation operator $\hat{C}_F^N$ is given by $\hat{C}_F^{F-N}$. Furthermore, the trivial rotations $\hat{C}_F^0$ and $\hat{C}_F^F$ are both equal to the identity operator $\hat{E}$. With the representation of the rotation operators $\hat{C}_F^N = \exp[-2\pi i N\hat{J}_z/F]$ in the basis $\{|jm\rangle\}$, the density matrix is written

$$\rho_{m'm}^{\text{des}} = \frac{1}{F}\sum_{N=0}^{F-1} \exp\left[\frac{2\pi i N}{F}(m'-m)\right]\rho_{m'm}^0, \qquad (17)$$

in terms of the reference density matrix $\rho_{m'm}^0$. The sum of exponential terms is identified as a geometric series and simplified to the Kronecker delta

$$\delta_{m'-m,nF} = \frac{1}{F}\sum_{N=0}^{F-1} \exp\left[\pm\frac{2\pi i N}{F}(m'-m)\right], \qquad (18)$$

with any integer n. Consequently, together with Eq. (15) the final expression for the density matrix of the desorbate is obtained

$$\rho_{m'm}^{\text{des}} = \sum_d \rho^0(m,d)\delta_{m'-m,d}\delta_{d,n[f,F]}, \qquad (19)$$

with the least common multiple $[f,F]$ of the foldnesses and an arbitrary integer n. Evidently, the local and the ensemble symmetry cause a sparse density matrix for the desorbing molecule ensemble: Its sub/superdiagonals are only nonzero if their index is a multiple of both the local and the ensemble foldness.

Ultimately, the orientation and aligment parameters Eq. (10) resulting from the density matrix of the desorbate ensemble Eq. (19) feature the following characteristic: Parameters the component of which does not correspond to the local and the ensemble foldness of the rotational symmetry become zero. The nonvanishing parameters are composed of equivalent contributions from the differently orientated molecule mixtures.

B. Reflection symmetry

If the point symmetry of the adsorbate includes a reflection symmetry, further constraints are imposed on the density matrix of the desorbate and thus the orientation and alignment parameters. The reflection symmetry possesses either local or ensemble characteristic (see Sec. II): In case of local symmetry, the desorbate ensemble shows the reflection symmetry of a single molecule adsorbed on the surface. Thus, the density operators $\hat{\rho}^N$ of the orientated molecule mixtures are intrinsically symmetric with respect to the reflection operation. Otherwise, the desorbate exhibits the ensemble symmetry with regard to two molecule mixtures that originate from mirrored equivalent adsorption sites. Then, the density operators of the orientated molecule mixtures themselves

$$\hat{\rho}^N = \tfrac{1}{2}(\hat{\rho}_1^N + \hat{\rho}_2^N) = \tfrac{1}{2}(\hat{\rho}_1^N + (\hat{\rho}_1^N)'), \qquad (20)$$

are composed of equivalent density operators $\hat{\rho}_1^N$ and $\hat{\rho}_2^N$ describing these two molecule mixtures. Since the two density operators are transformed into each other by the reflection operation, the density operators of the orientated molecule mixtures are again symmetric with regard to the reflection operation.

By way of example, for a mirror plane $\sigma(xz)$ the density matrices of the orientated molecule mixtures

$$(\rho_{m'm}^N)' = \langle jm'|\hat{\sigma}^\dagger(xz)\hat{\rho}^N\hat{\sigma}(xz)|jm\rangle, \qquad (21)$$

remain unchanged after the reflection operation. The reflection operator $\hat{\sigma}(xz) = \hat{C}_2(y)\hat{i}$ that is equivalent to an inversion $\hat{i}$ at the axes origin followed by a π rotation about the y axis is a self-adjoint and unitary operator. The matrix elements of the reflection operator

$$\langle jm'|\hat{\sigma}(xz)|jm\rangle = (-1)^{-m}\delta_{m',-m}, \qquad (22)$$

directly follow from the transformation properties of the basis states $\{|jm\rangle\}$.[22] With these matrix elements, the density matrices after the reflection operation result in

$$(\rho^N_{m'm})' = (-1)^{m'-m} \rho^N_{-m'-m}. \tag{23}$$

Due to the reflection symmetry, the transformed density matrices are equal to the original density matrices for all orientated molecule mixtures.

Equally, the density matrix of the desorbing molecule ensemble Eq. (17) is transformed into

$$(\rho^{\text{des}}_{m'm})' = \frac{1}{F} \sum_{N=0}^{F-1} \exp\left[-\frac{2\pi i N}{F}(m'-m)\right](\rho^0_{m'm})', \tag{24}$$

by the reflection operation. The sum of exponential terms is again reduced to the Kronecker delta Eq. (18). Moreover, the reflection operation leaves the reference density matrix unchanged. Then, the transformed density matrix of the desorbate ensemble

$$(\rho^{\text{des}}_{m'm})' = (-1)^{m'-m} \rho^{\text{des}}_{-m'-m}, \tag{25}$$

also remains unchanged after the reflection operation.

Finally, the orientation and alignment parameters after the reflection operation result in

$$A^{(k)}_q{}'(j) = (-1)^k (-1)^q A^{(k)}_{-q}(j) = (-1)^k A^{(k)}_q{}^*(j), \tag{26}$$

by inserting the transformed density matrix of the desorbate into Eq. (9) and applying the Wigner-Eckhardt theorem. Thus, each parameter transforms into its complex conjugate multiplied by an alternating sign for odd and even rank, repsectively. However, the transformed parameters are equal to the orignal parameters since the density matrix of the desorbate is not changed by the reflection operation. Consequently, the real part of the parameters vanishes for odd rank whereas the imaginary part becomes zero for even rank.

All symmetry considerations in Sec. IV exemplified with reference to the orientation and alignment parameters can equivalently be done for the state multipole moments. Since both the parameters and the moments identically transform like spherical tensors [see Eq. (11)], the analogous investigation for the state multipole moments leads to the same conclusions.

V. APPLICATION TO CO PHOTODESORBING FROM Cr₂O₃(0001)

In previous experiments,[31] the laser induced desorption of CO molecules from a $Cr_2O_3(0001)$ surface was investigated by quantum state resolved $(1+1')$ REMPI measurements via the CO $(B\,^1\Sigma^+ \leftarrow X\,^1\Sigma^+)$ transition. The adsorbed CO molecules were desorbed by an unpolarized laser ($\lambda_{\text{des}} = 193$ nm) incident along the surface normal z. The detection of the desorbed CO molecule ensemble was realized by a linearly polarized probe laser system ($\lambda = 115$ nm, $\lambda' = 345$ nm) running parallel to the surface. To characterize the rotational alignment of the desorbate ensemble, the quadrupole moment

$$A^2_0(j) = \frac{\langle 3\hat{J}^2_z - \hat{J}^2\rangle^{j\gg1}}{j(j+1)} = 2\langle P_2(\cos(\theta))\rangle, \tag{27}$$

was determined in the classical vector model:[22] In the limit of high j states, the discrete sum $\langle\rangle$ over the m states of the angular momentum projection $\hat{J}_z$ converges a continuous integral $\langle\rangle$ over $\cos\theta = J_z/J$ (see Sec. III). In this classical limit, the quadrupole moment ranges from -1 for pure cartwheel rotation ($\mathbf{J}\perp\mathbf{n}_z$) to $+2$ for pure helicopter rotation ($\mathbf{J}\|\mathbf{n}_z$) of the molecules. For this alignment investigation, only transitions of the R branch were employed. Probe laser light with polarization planes parallel and perpendicular to the surface normal led to the REMPI intensities $I_\|$ and $I_\perp$, respectively. Since the ionization step of the REMPI process was assumed to be saturated, the polarization anisotropy

$$R = \frac{I_\| - I_\perp}{I_\| + 2I_\perp} = -\frac{1}{2}\langle P_2(\cos(\theta))\rangle = -\frac{1}{4}A^2_0(j), \tag{28}$$

was directly related to the quadrupole moment A^2_0 for P and R branches in the classical limit of high j states.[21,32]

A preferential helicopter and cartwheel motion was observed for the desorbing CO molecules with weak and strong rotational excitation, respectively. This experimental finding was theoretically clarified by quantum mechanically evaluating the quadrupole moment of the desorbate ensemble within recent quantum dynamical wavepacket calculations.[33,34] The laser procured DIET process (desorption induced by electronic transitions)[35] was treated within a two state model. The employed three-dimensional (3D) potential energy surfaces (PESs) with the coordinates $\{z, \theta, \phi\}$ were obtained from embedded cluster *ab initio* calculations on configuration interaction (CI) level.[36,37] In these electronic structure calculations, the internal $CO(5\sigma \to 2\pi^*)$ excitation of the adsorbed molecule was assigned to the involved electronically excited state. The laser induced electronic transition was modeled as a Franck–Condon excitation of the rovibrational ground state to the electronically excited state. The relaxation of the electronic transition was described by a stochastic wave packet method including an incoherent averaging of all observables with respect to an exponential decay of the electronic excitation.[38,39] The subsequent time evolution in the electronic ground state was proceeded up to convergence of the desorbed wave packet part that was consecutively separated by a grid change method.[40]

These experimental and theoretical investigations of the photodesorption system $CO–Cr_2O_3(0001)$ are examples for the analysis of orientation and alignment in the dynamics of molecules on surfaces.[1–10,23–29] Like in the introduced experiments,[31] most experimental studies[2,3,5–10] generally assume a cylindrical symmetry about the surface normal z and consequently a strictly flat surface. Then, all off-axial parameters $A^{(k)}_q$ and moments $\rho^{(k)}_q$ with $q \neq 0$ become zero, respectively.[21] This assumption ensures that the measured apparent parameters and the real parameters coincide.[3] To our knowledge, the only experimental investigation beyond this simplification are the studies of the orientation of N_2 scattered from Ag(111) by Sitz *et al.*[1,4] In the associated alignment investigation, the imposed assumption of cylindrical symmetry is supported by a semiquantitative error estimate.[3]

However, in the corresponding theoretical studies[23–29] the real quadrupole moment Eq. (27) is directly evaluated

regardless of the apparent quadrupole moment that is measured in the experiments. Particularly, theoretically predicted signatures of reaction sites characterized by alignment features[29] have to be carefully compared to experimental results since the azimuthal environment violating the cylindrical symmetry depends on the specific site. In case of a remarkable violation of the cylindrical symmetry, the descriptions in experiment and theory lead to incomparable results. Hence, in the following we quantitatively scrutinize the assumption of the cylindrical symmetry for the CO molecule ensemble photodesorbing from $Cr_2O_3(0001)$ and thus the comparability of the already realized experimental and theoretical studies.[31,33,34] Moreover, this investigation provides an illustrative application of the symmetry analysis developed in the Sec. IV.

To discuss cylindrical symmetry for the experimental measurements of CO photodesorbing from $Cr_2O_3(0001)$, the laser induced desorption process and the subsequent REMPI detection have to be considered. The laser induced desorption process does not violate the cylindrical symmetry, since the normal incidence of the unpolarized desorption laser only singles out the surface normal z. The REMPI detection of the desorbate within a detection cone about the surface normal with half aperture angle of 30° is also in accord with the cylindrical symmetry.[41] For the employed $(1+1')$ REMPI process, the expression for the measured intensity

$$I = C_{det} N(j_i) \sum_{kq} P_q^{(k)}(j_i, \Lambda_i, j_e, \Lambda_e, \Omega) A_q^{(k)}(j_i), \quad (29)$$

holds for all cases of photon polarization and detection geometry.[21] The constant C_{det} contains several experimental factors (detector sensitivity, probe laser intensity, probe molecule density in the probe region, etc.). The population of the probed state j_i is denoted by $N(j_i)$. The quantities $P_q^{(k)}(j_i, \Lambda_i, j_e, \Lambda_e, \Omega)$ are the so-called line strength factors that include the characteristics of the involved states $\{j_i, \Lambda_i\}$, $\{j_e, \Lambda_e\}$ with orbital angular momentum Λ and the detection geometry given by the angle set Ω. The $(1+1')$ REMPI process is a two-photon process with an one-photon excitation and an one-photon ionization step. On account of the selection rules of optical transitions and the rules of angular momentum vector coupling, only orientation and aligment parameters up to rank $k=4$ are accessible by this process, which gives the general limit of the summation in Eq. (29).[42] For linearly polarized probe laser light, all orientation parameters (with odd rank) become zero. If the probe laser light is circularly polarized, the alignment parameters (with even rank) vanish. Only elliptically polarized probe laser light is sensitive to all parameters.[21]

In the experiments of interest, however, the ionization step is assumed to be saturated.[31] Thus, the REMPI process becomes independent of the ionization step and can be equivalently described as a one-photon process.[43] This simplified picture is confirmed by studies of D_2 desorbing from Cu(111) with a very similar $(1+1')$ REMPI detection scheme.[44] Due to the one-photon character, the REMPI detection with saturated ionization step is only sensitive to parameters up to rank $k=2$.[43,44] Because of the CO coverage of the well-ordered $Cr_2O_3(0001)$ surface in the submonolayer

regime, the adsorbed CO molecules have a statistically equilibrated local order. Consequently, the CO adsorbate shows a threefold ensemble symmetry (see Fig. 1). Since the desorption laser obeys cylindrical symmetry, this threefold symmetry is further imposed on the desorbing CO molecule ensemble. Following the symmetry consideration of Sec. IV, all parameters of the desorbate ensemble the component of which is not a multiple of three become zero. Ultimately, the measured REMPI intensity is cylindrically symmetric, since it does not contain off-axial parameters that are in accord with the threefold ensemble symmetry. Regarding the linearly polarized detection laser light, the only remaining parameters contributing to the REMPI intensity are $A_0^{(0)}$ and $A_2^{(0)}$. In conclusion, the analysis of the experimental data[31] was already correct due to the symmetry of the investigated system itself. The usual requirement of cylindrical symmetry for extracting the quadrupole moment was redundant.

To extend our consideration beyond the scope of the already realized experimental studies, henceforth orientation and alignment parameters up to rank $k=4$ are considered. These parameters could be measured by a real two-photon detection method like $(1+1)$ LIF without saturation or $(2+1)$ REMPI with saturated ionization step. The interpretation of the experimental data resulting from such more sophisticated detection scheme would greatly benefit from the following theoretical inspection.

The analysis of the angular momentum distribution of CO molecules photodesorbing from $Cr_2O_3(0001)$ is based on the introduced theoretical studies.[33,34] For the coordinates $\{z, \theta, \phi\}$ of the 3D PESs, the angles $\{\theta, \phi\}$ are associated with a Cartesian coordinate system with the x axis along the short line of two chromium surface ions (see Fig. 1). Within these coordinates, the CO adsorbate shows a local reflection symmetry with regard to the mirror plane $\sigma(xz)$ in addition to the threefold ensemble symmetry resulting in C_{3v} point symmetry. Again employing the symmetry consideration of Sec. IV reveals that $A_0^{(0)}$, $A_2^{(0)}$, $Im(A_3^{(3)})$, $A_4^{(0)}$, $Re(A_3^{(4)})$ are the only nonvanishing parameters up to rank $k=4$. The corresponding parameters with negative component are omitted, because of their direct dependence on the parameters with positive component [see Eq. (26)]. To determine orientation and alignment parameters for a specific j state within our quantum dynamical simulations, the populations of the m states are needed for the axial parameters whereas the coherence relation between the m states is necessary for the off-axial parameters (see Sec. III).

However, the access to the coherence information is impossible within the scope of the stochastic wave packet method originally used for describing the relaxation of the laser induced electronic excitation. Therefore, a simplified picture is employed: After the time evolution for a characteristic residence lifetime in the electronically excited state, the wave packet is instantaneously transferred to the electronic ground state. The characteristic residence lifetime $\tau = 36$ fs is chosen such that the quadrupole moment obtained from the original calculations including the stochastic wave packet method is reproduced.[33,34] This can be verified by Fig. 2 depicting the parameters $A_2^{(0)}$, $Im(A_3^{(3)})$, $A_4^{(0)}$, $Re(A_3^{(4)})$ as functions of the angular momentum j for the CO molecules
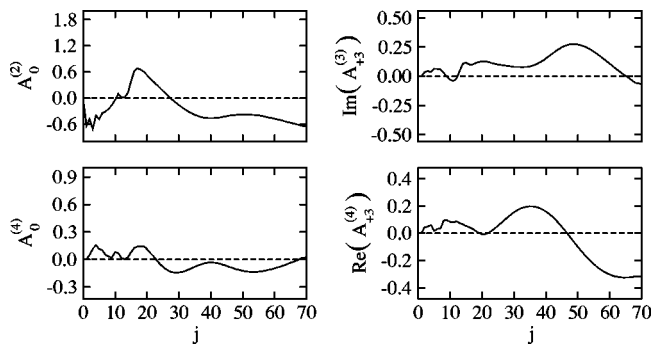
FIG. 2. Nonvanishing orientation and alignment parameters $A_q^{(k)}$ with $k = \{1,2,3,4\}$ as functions of angular momentum j for a threefold ensemble of CO molecules photodesorbing from $Cr_2O_3(0001)$.

photodesorbing from $Cr_2O_3(0001)$. The plot range of the angular momentum is limited by the highest angular momentum $j_{max} = 70$ that is populated for the asymptotic desorbate ensemble. Because of the renormalization of the populated j states for determining the parameters, the monopole moment $A_0^{(0)}$ has the trivial value of unity for all j states and is, therefore, omitted (see Sec. III). The plot range for the parameters given by

$$-1 \leq A_0^{(2)} \leq 2,$$
$$-\sqrt{5}/4 \leq \mathrm{Im}(A_3^{(3)}) \leq \sqrt{5}/4,$$
$$-3/7 \leq A_0^{(4)} \leq 1, \qquad (30)$$
$$-3\sqrt{105}/64 \leq \mathrm{Re}(A_3^{(4)}) \leq 3\sqrt{105}/64,$$

is the range of the parameters in the classical limit of high j states. This representation of the parameters is convenient to describe the preferential character of the rotational molecule motion depending on the angular momentum state j.[33,34] The polarization dependence of the parameters $\mathrm{Im}(A_3^{(3)})$, $A_4^{(0)}$, $\mathrm{Re}(A_3^{(4)})$ could be measured by a two-photon detection scheme and compared to the theoretical findings in Fig. 2.

The essential disentanglement of the real parameters included in the apparent parameters would strongly be simplified by the symmetry related vanishing of several parameters. Consequently, the measurements and the data analysis would be much more straightforward.

In order to decide on the significance of higher order terms with rank $k > 4$, the angular momentum distribution of the desorbing CO molecules is analyzed with respect to the polarization magnitude of the state multipole moments $\rho_q^{(k)}$. For the discussion of the polarization magnitude, the consideration of the orientation and alignment parameters would not be appropriate due to their complicated normalization that depends on both the rank k and the angular momentum state j [see Eq. (9)]. Therefore, we favor the state multipole moments Eq. (5) with their uniform normalization. To quantify the magnitude of the state multipole moments for the total angular momentum distribution, the polarization peaks

$$\pi_q^{(k)} = \max_j |\rho_q^{(k)}(j)|^2, \qquad (31)$$

over all populated j states are determined. Figure 3 shows the significant polarization peaks of the state multipole moments for a single CO molecule and an ensemble of CO molecules photodesorbing from $Cr_2O_3(0001)$. To resolve the occurring peaks, a logarithmic scale for the polarization magnitude is chosen. The upper limit of this scale is given by the trivial monopole peak $\pi_0^{(0)} = 1$ that results from the constant monopole moment $\rho_0^{(0)}(j) = 1$. The polarization peaks are shown up to rank $k = 12$ where their values are fallen off to a negligible magnitude of about 10^{-3}. For a single desorbing CO molecule (see left panel of Fig. 3), the axial polarization peaks $\pi_0^{(k)}$ with odd rank vanish due to the reflection symmetry: The axial moments $\rho_0^{(k)}$ are real quantities by definition. However, the mirror plane $\sigma(xz)$ causes the real parts of the moments $\rho_q^{(k)}$ with odd rank to become zero. Hence, the axial moments and peaks with odd rank vanish. Furthermore, the polarization peaks are symmetric with respect to their component $q \to -q$ since the direct relation of
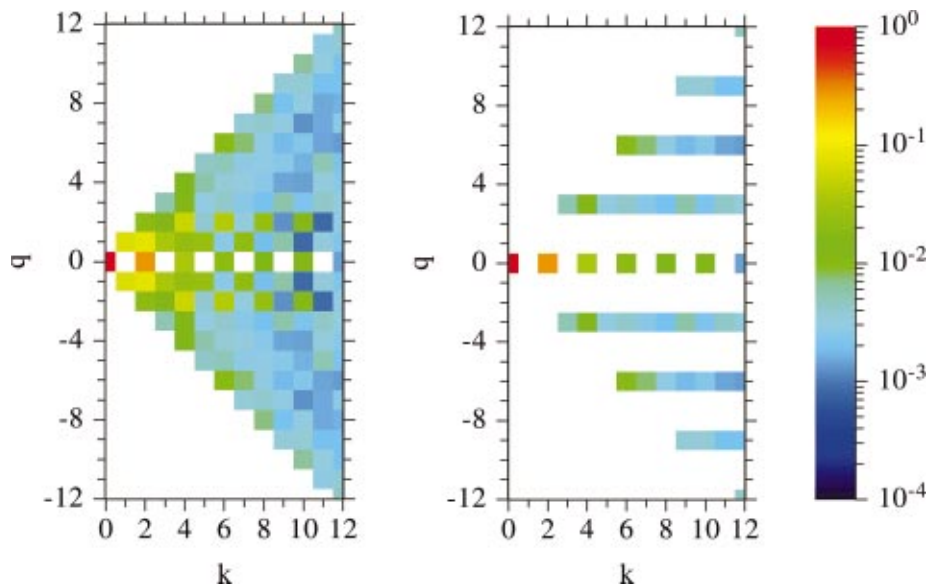

FIG. 3. (Color) Polarization peaks $\pi_q^{(k)}$ of the state multipole moments for CO photodesorbing from $Cr_2O_3(0001)$. The left graph shows the result for a single molecule whereas the right graph illustrates the result for a threefold molecule ensemble.

the orientation and alignment parameters with opposite components Eq. (26) is equivalently valid for the state multipole moments. The leading peaks in the state multipole expansion are the monopole peak $\pi_0^{(0)} = 1$ and the quadrupole peak $\pi_0^{(2)} = 0.274$. The next following peaks $\pi_1^{(2)}$, $\pi_1^{(1)}$, $\pi_2^{(4)}$, $\pi_2^{(6)}$, $\pi_0^{(4)}$, $\pi_1^{(3)}$ are between three and eight times smaller than the quadrupole peak. All remaining peaks are smaller than the quadrupole peak by one or more orders of magnitude. For a desorbing CO molecule ensemble (see right panel of Fig. 3), off-axial moments and peaks are additionally canceled if their component is not consistent with the threefold ensemble symmetry. Then, the off-axial peaks $\pi_1^{(2)}$, $\pi_1^{(1)}$, $\pi_2^{(4)}$, $\pi_2^{(6)}$, $\pi_1^{(3)}$ become zero. Consequently, all peaks with rank $k > 4$ are smaller than the quadrupole peak by at least one order of magnitude. Finally, the angular momentum distribution of the CO molecule ensemble photodesorbing from $Cr_2O_3(0001)$ is sufficiently described by the axial state multipole moments $\rho_0^{(0)}$, $\rho_0^{(2)}$, $\rho_0^{(4)}$ and the small off-axial corrections $Im(\rho_3^{(3)})$, $Re(\rho_3^{(4)})$. In conclusion, the characteristics of the orientation and alignment parameters in Fig. 2 represent a nearly complete description of the angular momentum distribution. Moreover, the experiments proposed above employing a two-photon detection scheme would also provide an almost entire picture that could be compared to the theoretical results.

VI. CONCLUSIONS

In order to analyze the angular momentum distribution of molecules desorbing from a surface, we demonstrated that the complete point symmetry of the surface is introduced to adsorbates of statistically equilibrated order. Since the desorption process generally respects the point symmetry imposed on the adsorbate, we concluded that this symmetry is further adopted to the desorbate and thus to the angular momentum distribution of the desorbing molecules. The symmetry restricted angular momentum distribution was revealed to become sparse by vanishing of several terms that are not consistent with the imposed point symmetry. For the sparse angular momentum distribution, we completely derived the resulting symmetry consistent orientation and alignment parameters.

Previous experimental studies on the alignment of CO molecules photodesorbing from a $Cr_2O_3(0001)$ surface were theoretically analyzed with regard to the C_{3v} point symmetry of the surface. Due to the resulting sparse angular momentum distribution of the desorbing CO molecules, the measured apparent quadrupole moment could be identified as the real quadrupole moment. From the theoretically determined angular momentum distribution, we predicted the dependence of all nonzero orientation and alignment parameters up to rank $k = 4$ on the angular momentum state. These parameters were proved to dominate the angular momentum distribution by additonally evaluating polarization peaks even for all higher-order terms. Finally, we proposed a more refined experimental reinvestigation of the photodesorption system $CO-Cr_2O_3(0001)$ to reproduce the predictions resulting from our complete theoretical description of the angular momentum distribution of the desorbate.

[1] G. O. Sitz, A. C. Kummel, and R. N. Zare, J. Chem. Phys. **87**, 3247 (1987).
[2] D. C. Jacobs, K. W. Kolasinski, R. J. Madix, and R. N. Zare, J. Chem. Phys. **87**, 5038 (1987).
[3] G. O. Sitz, A. C. Kummel, and R. N. Zare, J. Chem. Phys. **89**, 2558 (1988).
[4] G. O. Sitz, A. C. Kummel, R. N. Zare, and J. C. Tully, J. Chem. Phys. **89**, 2572 (1988).
[5] D. C. Jacobs, K. W. Kolasinski, S. F. Shane, and R. N. Zare, J. Chem. Phys. **91**, 3182 (1989).
[6] D. Wetzig, R. Dopheide, M. Rutkowski, R. David, and H. Zacharias, Phys. Rev. Lett. **76**, 463 (1996).
[7] D. Wetzig, M. Rutkowski, R. David, and H. Zacharias, Europhys. Lett. **36**, 31 (1996).
[8] H. Hou, S. J. Gulding, C. T. Rettner, A. M. Wodtke, and D. J. Auerbach, Science **277**, 80 (1997).
[9] D. Wetzig, M. Rutkowski, W. Etterich, R. David, and H. Zacharias, Surf. Sci. **402–404**, 232 (1998).
[10] M. Rutkowski, D. Wetzig, and H. Zacharias, Phys. Rev. Lett. **87**, 246101 (2001).
[11] *Applied Laser Spectroscopy. Techniques, Instrumentation, and Applications*, edited by D. L. Andrews (VCH, New York, 1992).
[12] A. C. Kummel, G. O. Sitz, and R. N. Zare, J. Chem. Phys. **85**, 6874 (1986).
[13] A. C. Kummel, G. O. Sitz, and R. N. Zare, J. Chem. Phys. **88**, 6707 (1988).
[14] A. C. Kummel, G. O. Sitz, and R. N. Zare, J. Chem. Phys. **88**, 7357 (1988).
[15] *International Tables for Crystallography, Vol. A: Space Group Symmetry*, edited by T. Hahn (Reidel, Dordrecht, 1983).
[16] M. Hamermesh, *Group Theory and its Application to Physical Problems* (Addison-Wesley, Reading, MA, 1964).
[17] G. Burns, *Introduction to Group Theory with Applications* (Academic, New York, 1977).
[18] C. Xu, B. Dillmann, H. Kuhlenbeck, and H.-J. Freund, Phys. Rev. Lett. **67**, 3551 (1991).
[19] M. Bender, D. Ehrlich, I. N. Yakovkin, F. Rohr, M. Bäumer, H. Kuhlenbeck, H.-J. Freund, and V. Staemmler, J. Phys.: Condens. Matter **7**, 5289 (1995).
[20] K. Blum, *Density Matrix Theory and Application* (Plenum, New York, 1981).
[21] A. J. Orr-Ewing and R. N. Zare, Annu. Rev. Phys. Chem. **45**, 315 (1994).
[22] R. N. Zare, *Angular Momentum. Understanding Spatial Aspects in Chemistry and Physics* (Wiley, New York, 1988).
[23] J. Dai and J. C. Light, J. Chem. Phys. **108**, 7816 (1998).
[24] D. A. McCormack, G.-J. Kroes, R. A. Olsen, E.-J. Baerends, and R. C. Mowrey, J. Chem. Phys. **110**, 7008 (1999).
[25] A. Eichler, J. Hafner, A. Gross, and M. Scheffler, Chem. Phys. Lett. **311**, 1 (1999).
[26] A. Gross and M. Scheffler, Phys. Rev. B **61**, 8425 (2000).
[27] M. Rutkowski and H. Zacharias, Phys. Chem. Chem. Phys. **3**, 3645 (2001).
[28] A. Dianat and A. Gross, Phys. Chem. Chem. Phys. **4**, 4126 (2002).
[29] M. F. Somers, D. A. McCormack, G.-J. Kroes, R. A. Olsen, E.-J. Baerends, and R. C. Mowrey, J. Chem. Phys. **117**, 6673 (2002).
[30] N. E. Shafer-Ray, A. J. Orr-Ewing, and R. N. Zare, J. Phys. Chem. **99**, 7591 (1995).
[31] I. Beauport, K. Al-Shamery, and H.-J. Freund, Chem. Phys. Lett. **256**, 641 (1996).
[32] C. H. Greene and R. N. Zare, Annu. Rev. Phys. Chem. **33**, 119 (1982).
[33] S. Thiel, M. Pykavy, T. Klüner, H.-J. Freund, R. Kosloff, and V. Staemmler, Phys. Rev. Lett. **87**, 077601 (2001).
[34] S. Thiel, M. Pykavy, T. Klüner, H.-J. Freund, R. Kosloff, and V. Staemmler, J. Chem. Phys. **116**, 762 (2002).
[35] *Desorption Induced by Electronic Transitions, DIET, Vol. 1*, edited by N.

H. Tolk, M. M. Traum, J. C. Tully, and T. E. Madey (Springer-Verlag, Berlin, 1983).

[36] M. Pykavy, V. Staemmler, O. Seiferth, and H.-J. Freund, Surf. Sci. **479**, 11 (2001).

[37] M. Pykavy, S. Thiel, and T. Klüner, J. Phys. Chem. B **106**, 12556 (2002).

[38] J. W. Gadzuk, L. J. Richter, S. A. Buntin, D. S. King, and R. R. Cavanagh, Surf. Sci. **235**, 317 (1990).

[39] J. W. Gadzuk, Surf. Sci. **342**, 345 (1995).

[40] R. Heather and H. Metiu, J. Chem. Phys. **86**, 5009 (1987).

[41] S. Borowski, T. Klüner, H.-J. Freund, I. Klinkmann, K. Al-Shamery, M. Pykavy, and V. Staemmler, Appl. Phys. A (to be published).

[42] D. C. Jacobs and R. N. Zare, J. Chem. Phys. **85**, 5457 (1986).

[43] R. Altkorn and R. N. Zare, Annu. Rev. Phys. Chem. **35**, 265 (1984).

[44] H. Hou, S. J. Gulding, C. T. Rettner, A. M. Wodtke, and D. J. Auerbach, J. Electron Spectrosc. Relat. Phenom. **98−99**, 133 (1999).